Differences in the phosphate oxygen requirements for self-cleavage by the extended and prototypical hammerhead forms

Olivera Mitrasinovic and Lloyd M. Epstein[1],*

Department of Chemistry and [1]Department of Biological Science, Florida State University, Tallahassee, FL 32306-3050, USA

ABSTRACT

The hammerhead self-cleaving motif occurs in a variety of RNAs that infect plants and consists of three non-conserved helices connected by a highly conserved central core. A variant hammerhead, called the extended hammerhead, is found in satellite 2 transcripts from a variety of caudate amphibians. The extended hammerhead has the same core as the prototypical hammerhead, but has unusually conserved sequence and structural elements in its peripheral helices. Here we present the results of a thiophosphate substitution interference analysis of the *pro-R*p phosphate oxygen requirements in the two hammerhead forms. Five *pro-R*p phosphate oxygens, all in the central core, were found to be important for self-cleavage by the prototypical hammerhead. A similar set of core positions were important for self-cleavage by the extended hammerhead, but five non-core positions were also found to be important. Thiosubstitution at one of these positions had the most severe effect on self-cleavage observed in this analysis. Mn^{2+} did not alleviate this negative effect, indicating that this position was not part of a divalent cation binding site. We propose that novel tertiary interactions in the extended hammerhead help form the same catalytic core structure as that used by the prototypical plant virus hammerhead.

INTRODUCTION

One of the smallest and most intensively studied catalytic RNA motifs is the self-cleaving hammerhead domain. Hammerheads were first identified in a comparison of the sequences surrounding the sites of self-cleavage in the virusoid of lucerne transient streak virus, the satellite of tobacco ringspot virus and the avocado sunblotch viroid (1) and have since been found in a diverse array of plant viroids, virusoids and viral satellite RNAs (2). As originally proposed, the structural model of the consensus hammerhead consists of three base paired stems that emanate from a highly conserved single-stranded core (Fig. 1A). This model has received strong support from mutational studies

(reviewed in 3) and is consistent with the three-dimensional structures of several hammerhead variants that were solved by physical techniques such as fluorescence resonance energy transfer (4) and X-ray crystallography (5,6). Despite an abundance of structural data, however, the details of the cleavage mechanism remain to be determined (reviewed in 7). The reaction involves nucleophilic attack on the phosphodiester at the cleavage site by the adjacent 2′-OH. The only requirement for the reaction is a divalent metal cation, which is probably involved in extracting the proton from the 2′-OH, but may also help stabilize the pentacoordinated reaction intermediate or the leaving groups. The problem with assigning specific functions to the divalent cations is that it is not clear how many ions are required for catalysis and where the catalytically important cations bind in the active structure. The stringent sequence requirements in the single-stranded central core (8), the clustering of important functional groups in this core (9–14) and the absence of sequence specificity in the helical regions (reviewed in 3) suggest that the catalytically important features of the hammerhead are all located in the conserved core.

To complement analysis of the self-cleaving plant virus hammerheads, we have studied self-cleavage by transcripts of a highly repetitive DNA called satellite 2, which has been found in six families of caudate amphibians (15–18). Conserved features of satellite 2 include: its ~330 bp repeat length (15,17); the fact that it is transcribed in all tissues investigated (15,17,19); its transcriptional promoter, which is similar to and interchangeable with promoters normally associated with a subset of small nuclear RNA (snRNA) genes (16,20); the ability of satellite 2 transcripts to catalyze their own site-specific cleavage (16,18,21). The function or significance of this novel genetic element is not presently known, but on the basis of the similarities between its characteristics and those of certain other repetitive DNA sequences, we proposed that satellite 2 is a proliferative retroposable element derived from a normal cellular snRNA gene (20).

Self-cleavage by satellite 2 transcripts occurs within a domain that is similar to the plant hammerhead, but the peripheral stems of the satellite 2 hammerhead have unusual and highly conserved features (Fig. 1B). Because the minimal active structure contains an elongated stem I region, we refer to this structure as the 'extended' hammerhead (22). Mutational studies demonstrated that sequences in the internal stem I loop and the external stem II

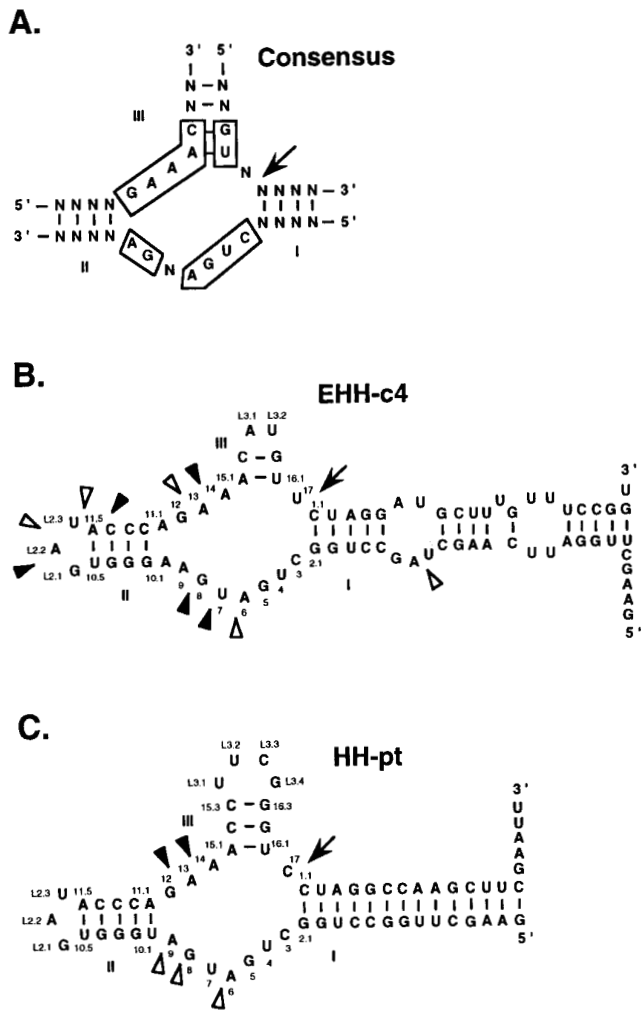*To whom correspondence should be addressed. Tel: +1 904 644 4560; Fax: +1 904 644 0481; Email: epstein@bio.fsu.edu

Figure 1. Hammerhead structures. (**A**) Consensus sequence and secondary structure of the self-cleaving hammerhead domain as proposed by Forster and Symons (1). Stems are numbered I–III; conserved nucleotides are boxed; the arrow denotes the site of cleavage. (**B**) Potential extended hammerhead structure in EHH-c4 transcripts. Nucleotides are numbered according to established conventions (42) and positions of important *pro-R*p phosphate oxygens identified in this study are indicated by arrowheads. White arrowheads indicate positions with relative intensity ratios between 1 and 2 SD above the mean of all positions; black arrowheads indicate positions with relative intensity ratios >2 SD above the group mean. (**C**) Potential hammerhead structure in HH-pt transcripts. Conventions are as in (B).

loop were important for cleavage (22,23). Of particular significance was the finding that these requirements are context specific, meaning that the internal stem I loop from one species was not always compatible with a stem II region from another species (23). Functional and comparative studies have resulted in the identification of two naturally occurring extended hammerhead designs that differ in the sequence and structural details of their stem I and stem II regions (18). Group A extended hammerheads, which are characterized by a 3 nt external stem II loop, occur in the family Salamandridae and are exemplified by the well-characterized hammerhead from *Notophthalmus viridescens* (21,22). Group B extended hammerheads, recognized by their 6 nt external stem II loops, occur in all other salamander families that have been investigated (17,18).

In previous studies, over 30 mutations in peripheral regions of the extended hammerhead abolished or severely inhibited self-cleavage (22,23). Although these results suggested that the peripheral regions had important roles in promoting catalysis or in helping to stabilize the active structure, we could not completely rule out the possibility that each of the mutations disrupted activity by promoting the formation of inactive RNA conformations (24,25). An alternative mechanism for identifying important functional groups in RNA that has less complicating effects than mutagenesis is to test the activity of RNAs that contain chemically modified nucleotides (26). In this report we describe a thiophosphate substitution interference analysis that was designed to identify phosphate oxygens in the extended hammerhead that are important for catalysis. In addition to phosphate oxygens in the conserved core that are known to be important for all hammerhead forms, we found several phosphate oxygens in peripheral regions of the extended hammerhead that were also important for self-cleavage. These results are consistent with the conclusions from previous mutation studies and provide direct evidence for the existence of specific and unique requirements in peripheral structures of the extended hammerhead.

MATERIALS AND METHODS

Materials

Restriction enzymes were purchased from New England Biolabs, SP6 RNA polymerase was from Epicenter Technologies, T4 polynucleotide kinase was from Promega, [γ-^{32}P]ATP was from New England Nuclear, *S*p stereoisomers of nucleoside 5′-(α-thio)-triphosphates (NTPαS) were from Amersham and iodoethanol was from Fisher Scientific.

Clones

EHH-c4 transcripts were transcribed from clone pC4, which was constructed previously and consists of the hammerhead domain from the *N.viridescens* clone pG47 with three substitutions in the stem III region that mimic the hammerhead domain from *Ambystoma talpoideum* (23). HH-pt transcripts were transcribed from clone pPt, which was constructed by mutation of A10.1 to T in the parent construct, pGES1 SLI (22). HH-NecO transcripts were transcribed from pNecO, which was constructed by mutation of the *Necturus maculosus* genomic clone pNmac7 (18) so that the encoded hammerhead had the sequence of the *Necturus* ovarian satellite 2 transcripts (Y.Zhang, S.R.Coats and L.M.Epstein, unpublished data).

In vitro transcription reactions

Internally labeled transcripts for kinetic measurements were prepared in 10 μl reactions consisting of 2 μg linearized plasmid DNA, 40 mM Tris–HCl, pH 7.5, 6 mM MgCl$_2$, 5 mM spermidine, 10 mM DTT, 250 μM (each) ATP, GTP and CTP, 5 μM UTP, 10 μCi [α-^{32}P]UTP and 25 U SP6 RNA polymerase. After incubation for 60 min at 20°C, radiolabeled transcripts were purified from unincorporated label by chromatography through Sephadex G-50. Full-length transcripts were purified from 10% polyacrylamide–7 M urea gels as described previously (21).

For the preparation of 5′-end-labeled, partially thiosubstituted transcripts, the labeled nucleotide was omitted from the transcription mixture, the concentration of each NTP was raised to 250μM and an amount of one specific NTPαS was added that resulted in

a majority of monosubstituted transcripts as determined by the generation of uniform band intensities after cleavage with iodine (see below). For ATPαS and GTPαS, these amounts gave NTP:NTPαS ratios that were equal to the number of occurrences of the nucleotide in the full-length transcript. This indicates that, as previously reported for transcription by T7 RNA polymerase (9,27), SP6 RNA polymerase did not differentiate between the normal and the thiosubstituted nucleotides during transcription. However, the optimal concentrations of CTPαS and UTPαS were approximately five times greater than those predicted by this ratio. Thus, the concentrations of thiosubstituted nucleotides that were used for the production of EHH-c4 transcripts were 14 µM ATPαS, 11 µM GTPαS, 89 µM CTPαS and 55 µM UTPαS. For the production of partially substituted HH-pt transcripts, 15 µM ATPαS, 12.5 µM GTPαS, 78 µM CTPαS and 83 µM UTPαS were optimal. After incubation for 60 min at 23°C, transcription products were dephosphorylated with calf intestinal alkaline phosphatase and 5′-end-labeled with T4 polynucleotide kinase and [γ-^{32}P]ATP as previously described (21). Full-length transcripts were separated from unincorporated label and purified as described above.

Self-cleavage kinetics

Transcripts were heated at 80°C for 5 min in 1 mM EDTA, pH 8.0, immediately chilled in ice/water and combined with 2 vol prewarmed buffer to initiate self-cleavage. Self-cleavage reaction mixtures (6 µl) consisted of 0.1–0.2 nM transcripts, 133 mM MES buffer, pH 6.9, 30 mM MgCl₂, 10 mM NaCl and 0.3 mM EDTA. After incubation at 42°C for the indicated times, 6 µl gel loading buffer (80 mM EDTA, 75% formamide, 0.05% xylene cyanol, 0.05% bromophenol blue) were added to stop the reactions. Transcripts and cleavage products were separated by electrophoresis through denaturing polyacrylamide gels and dried gels were quantified with a Betascope 603 Blot Analyzer (Betagen Corp.). First order rate constants (k) and reaction end-points (EP) were determined by non-linear least square fits of the data to the equation $F = EP\,(1 - e^{-kt})$, where F is equal to the fraction cleaved at time t (28).

Analysis of thiophosphate-substituted transcripts

Gel-purified, 5′-end-labeled, partially thiosubstituted transcripts were pooled and subjected to self-cleavage conditions in the presence of either 30 mM MgCl₂ or 30 mM MnCl₂ for a time sufficient to give ~50% cleavage. Cleavage products were separated by electrophoresis on 10% acrylamide–7 M urea gels and uncleaved transcripts and 5′-cleavage products were purified from gel slices as described (21). After precipitation with ethanol, RNA fractions were resuspended in 1 mM EDTA. Just prior to initiation of the iodoethanol reactions, 2 µl RNA (0.002–0.004 ng) were heated at 80°C for 1 min and chilled on ice. Sulfur-specific cleavage was initiated by the addition of 1 µl of a 25% solution of 2-iodoethanol in 95% ethanol. After incubation for 2 min at 90°C, reactions were stopped by adding an equal volume of stop buffer (80% formamide, 0.05% xylene cyanol, 0.05% bromophenol blue) on ice. Reaction products were separated on 12% polyacrylamide–7 M urea gels. 5′-End-labeled transcripts were also subjected to alkaline hydrolysis to generate standards for identification of the iodine cleavage products by

mixing 2 µl RNA (0.002–0.004 ng) with 2 µl 100 mM Na₂CO₃/NaHCO₃, pH 9.0, and boiling for 4 min.

Thiophosphate quantitative analysis

Autoradiographs were scanned on a SM3 scanner with 63.5 µm resolution (Howtek Inc.) and relative band intensities were determined by means of PDI Quantity One software (version 2.2). The relative band intensity is a measure of the intensity of a band relative to the intensity of the entire section of the lane analyzed. For each position, the relative intensity ratio was then calculated as the relative intensity of the band in the uncleaved fraction divided by the relative intensity of the band in the cleaved fraction. The bar graphs show plots of the average relative intensity ratios and their standard deviations, from a minimum of three independent experiments. For each combination of transcript and divalent cation, average relative intensity ratios were used to calculate an overall group mean and a group standard deviation after elimination of outliers from a normal distribution function using SPLUS software (Statistical Sciences Inc.). Potentially important positions were classified as exhibiting relative intensity ratios 1 or 2 SD above the group mean.

RESULTS

EHH-c4 and HH-pt transcripts

EHH-c4 transcripts were chosen to represent the extended hammerhead in the thiophosphate substitution interference analysis (Fig. 1B). The template for these transcripts was constructed previously and consists of the hammerhead domain from *N.viridescens* with the *A.talpoideum* stem III region (23). Figure 2A shows that self-cleavage by these transcripts fits well to the first order rate equation ($r^2 = 0.98$). The rate constant determined from this data, 0.039/min, is 5-fold greater than that of any naturally occurring extended hammerhead and we reasoned that the relatively high activity of EHH-c4 transcripts would facilitate our analysis and provide a greater level of sensitivity for identifying positions that were important but not absolutely critical for self-cleavage.

HH-pt transcripts closely resemble EHH-c4 transcripts but have modifications that make them look and behave more like a prototypical hammerhead (Fig. 1C). A 4 nt insertion in the apex of stem III stabilizes the stem III structure and eliminates the requirement for the internal loop in stem I (22). To ensure that the role of the internal loop in stem I was eliminated in HH-pt transcripts, the distal portion of stem I was replaced with a perfectly base paired non-homologous extension. Finally, so that the configuration would conform to that of the vast majority of naturally occurring plant hammerheads (2), A10.1 was changed to U, forming a base pair at the junction between stem II and the conserved core. Figure 2 shows that despite these modifications, HH-pt transcripts cleave with kinetics similar to those of EHH-c4 transcripts.

Thiophosphate substitution interference analysis

Phosphorothioate linkages were incorporated into the EHH-c4 and HH-pt transcripts during *in vitro* transcription by use of commercially available *S*p-NTPαS diastereomers as substrates. Transcription by SP6 RNA polymerase results in an inversion of configuration and the substitution of sulfur atoms in the *R*p configuration for non-bridging phosphate oxygens (26,29).
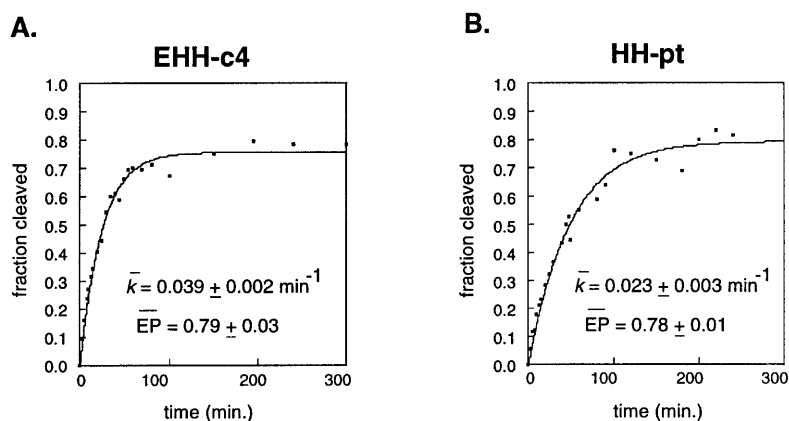
Figure 2. Self-cleavage of (**A**) EHH-c4 transcripts and (**B**) HH-pt transcripts. Internally labeled transcripts were cleaved in the presence of 30 mM Mg^{2+} at concentrations of 0.1–0.2 nM. The curves represent the data fitted to the equation $F = EP (1 - e^{-kt})$ as described in Materials and Methods. The first order rate constants (k) and reaction end-points (EP) given are the averages from three (EHH-c4) and two (HH-pt) independent experiments.

Ratios of NTP and NTPαS precursors were empirically determined that gave, on average, one phosphorothioate linkage per transcript. If a particular phosphate oxygen is important for cleavage, the substitution of a sulfur atom for that oxygen will inhibit cleavage and that substitution will be enriched in the uncleaved fraction. The occurrence of thiophosphate substitutions at specific positions in uncleaved full-length transcripts and 5′-cleavage fragments was determined by electrophoretic separation of iodoethanol-treated transcripts (26). Because the primary purpose of this study was to obtain evidence for fundamental differences between the extended and prototypical hammerheads, the analysis was designed to examine a large sample of *pro-R*p phosphate oxygens in the most efficient manner possible. Restriction of the analysis to regions upstream from the cleavage site permitted the use of a single and consistent 5′-end-labeling protocol. Nucleotides near the cleavage site were excluded from the analysis because the heavily labeled 5′-self-cleavage fragment made it difficult to quantify bands representing iodine cleavage at those positions. Nucleotides near the 5′-ends were also excluded because electrophoretic run times that gave the best separation of the larger bands typically caused the smaller bands to migrate off the gels.

Figure 3 shows examples of the analysis of *pro-R*p oxygens adjacent to A residues in the prototypical and extended hammerheads. In lanes 2 and 3 a more or less uniform distribution of bands resulting from iodine cleavage 5′ to A residues in EHH-c4 transcripts is evident in both the cleaved and uncleaved fractions. Four additional bands occur in these same lanes, corresponding to cleavage at positions C2.4, G2.2, G5 and G8. These are pronounced examples of non-specific cleavages that occurred sporadically throughout our experiments. Cleavage at these particular positions occurred when transcripts were heated in the absence of iodine (data not shown) and bands corresponding to cleavage at these positions were occasionally enriched in the alkaline hydrolysis standards (lane 1). Moreover, the extent of cleavage at these positions was highly variable between experiments and was typically less apparent when self-cleavage reactions were performed in the presence of Mn^{2+} (lanes 4 and 5). Cleavages at these positions occurred to a lesser extent with transcripts with G substitutions and were undetectable with either C or U substitutions. Although there was no way to control these and similar iodine-independent cleavages, their effect on our

calculations was diminished by averaging multiple, independent experiments. In fact, even though these particular bands appeared or didn't appear in unison, one of these positions, G8, was ultimately judged to be important for self-cleavage, while the others were judged to be unimportant (see below). Thus, the sporadic occurrence of iodine-independent cleavage did not affect our ability to differentiate between important and unimportant positions.

Most of the bands representing bona fide iodine-mediated cleavage of EHH-c4 transcripts were equally represented in the cleaved and uncleaved fractions, which indicates that most ATPαS substitutions did not affect self-cleavage (Fig. 3, lanes 2 and 3). Nevertheless, several positions were identified that did not fit this pattern. A9 and AL2.2 in EHH-c4 are particularly striking examples of positions where sulfur substitutions resulted in dramatic enrichment of bands in the uncleaved fractions. In other cases, the effects of thiophosphate substitutions were slight and became evident only after the data were quantified. For this purpose, the autoradiograms were scanned, band intensities were determined and relative intensity ratios were calculated as the ratio of the relative intensity of a band in the uncleaved fraction to the relative intensity of the same band in the cleaved fraction (see Materials and Methods). To determine the variability between experiments and to get better estimates of true intensity ratios, we averaged relative intensity ratios from a minimum of three independent experiments.

Figure 4 shows the compiled results for substitutions at all four nucleotides of the extended EHH-c4 transcripts when self-cleavages were performed in the presence of Mg^{2+} (white bars). For most positions, relative intensity ratios were fairly consistent between experiments. Ten of the 41 positions analyzed had mean relative intensity ratios that were ≥1 SD above the group mean (see Fig. 1B for a summary of these results). The *pro-R*p phosphate oxygens adjacent to A9, A13 and A14 in the central core were previously found to be important for self-cleavage in a thiophosphate substitution analysis of a prototypical hammerhead (9). Phosphate oxygens adjacent to U7 and G8, although not identified in the previous analysis, are also located in the highly conserved central core. The other phosphate oxygens implicated as important in the present analysis, adjacent to A2.7, AL2.2, UL2.3, A11.5 and C11.4, lie outside the central core and have not been implicated as important in any previous studies of prototypical hammerheads.
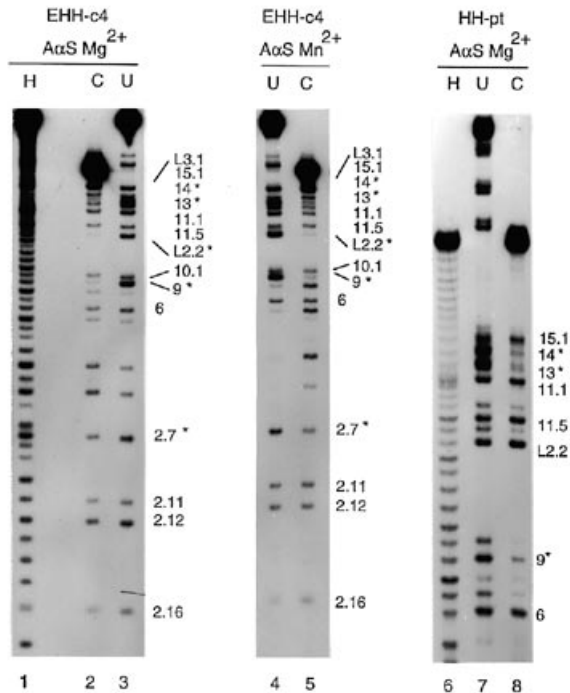
Figure 3. Thiophosphate substitution interference experiments with EHH-c4 and HH-pt transcripts. Examples are shown for the analysis of *pro-R*p phosphate oxygens 5′ to adenosine residues. The indicated transcripts were prepared using ATPαS precursors, 5′-end labeled and allowed to undergo self-cleavage in the presence of Mg^{2+} (lanes 2, 3, 7 and 8) or Mn^{2+} (lanes 4 and 5). Uncleaved reactants (U) and 5′-cleavage products (C) were isolated and individually treated with iodoethanol. The autoradiographs show electrophoretic separation of the products of the iodoethanol treatments. Parallel samples of transcripts subjected to alkaline hydrolysis (H) were included on the gels to facilitate identification of the products. Bands representing iodoethanol-mediated cleavages adjacent to adenosine residues are labeled according to the conventions presented in Figure 1. Unlabeled bands, which represent cleavages adjacent to unsubstituted positions, were not dependent on iodoethanol treatment and are further discussed in the text. Asterisks indicate positions of *pro-R*p phosphate oxygens that were judged to be important for self-cleavage by criteria described in the text and Figure 4.

Although the measured effects of substitutions at some of these positions are small, the effects of the sulfur substitutions adjacent to C11.4 in stem II and AL2.2 in the external loop of stem II equal or exceed the effects of thiophosphate substitutions at positions judged to be important in previous analyses of a variety of catalytic RNAs (9,27,30).

The compiled results for thiophosphate substitutions in HH-pt transcripts are shown in Figure 5. In general, a smaller number of positions were found to be important for cleavage by HH-pt transcripts and those that were found had smaller relative intensity ratios than those determined for important positions in the EHH-c4 transcripts (note the difference in the *y*-axis scales in Figs 4 and 5). Only five positions had ratios ≥1 SD above the group mean and all of these were in the conserved core. As in EHH-c4 transcripts, these included A13, A14 and three positions in the lower portion of the core, although these latter positions were shifted slightly towards stem II (Fig. 1C). Whether or not the base pair between A11.1 and U10.1 had a role in promoting this shift is not known, but it is clear that similar positions in the
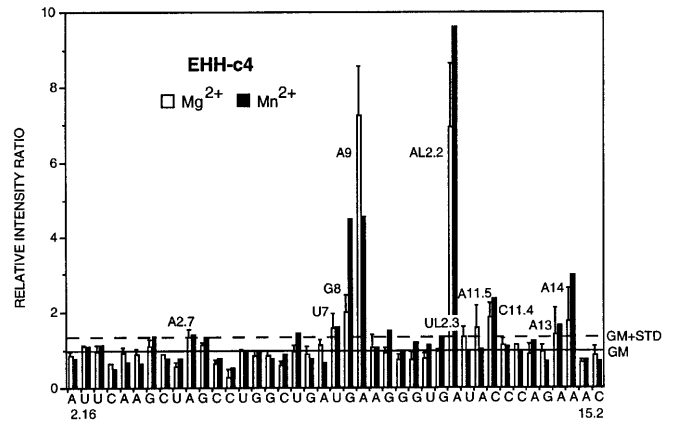

Figure 4. Relative intensity ratios of thiophosphate substitutions in EHH-c4 transcripts. Thiosubstituted transcripts were analyzed after self-cleavage in the presence of either 30 mM Mg^{2+} (white bars) or 30 mM Mn^{2+} (black bars) and relative intensity ratios were calculated for every *pro-R*p phosphate oxygen from A2.16 in stem I to C15.2 in stem III. The mean for each position was calculated from a minimum of three independent experiments. For clarity, standard deviations are shown only for transcripts cleaved in the presence of Mg^{2+}. The solid line at 1.00 represents the group mean (GM) of all positions after cleavage in the presence of Mg^{2+} and was calculated after elimination of A9, AL2.2 and C2.4, which were determined to be outliers of a normal distribution function of the data. The dashed line at 1.34 is 1 SD above the group mean and was used as our criteria for identifying positions where thiophosphate substitutions interferred with self-cleavage.
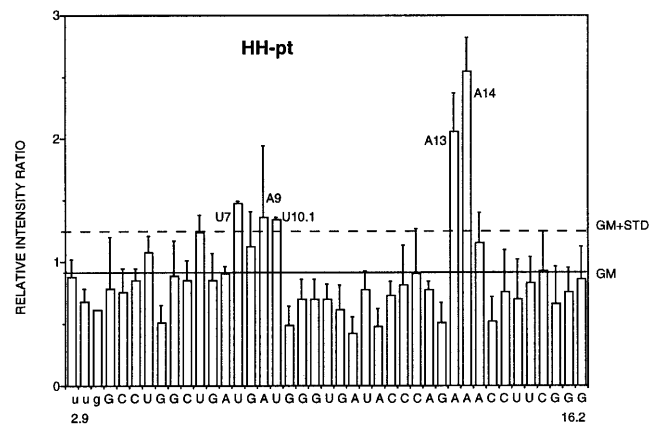

Figure 5. Relative intensity ratios of thiophosphate substitutions in HH-pt transcripts. The average relative intensity ratio and 1 SD from a minimum of three independent experiments is shown for each position from U2.9 in stem I to G16.2 in stem III. Values are shown only for transcripts analyzed after self-cleavage in the presence of 30 mM Mg^{2+}. The solid line at 0.89 is the group mean (GM) and the dashed line at 1.30 is 1 SD above the group mean.

conserved core are important for self-cleavage by both hammer-head forms. It is also clear that requirements for *pro-R*p phosphate oxygens in the peripheral regions of these hammerheads are very different.

Cleavage of thiophosphate-substituted transcripts in the presence of manganese

If the function of a phosphate oxygen is to coordinate a divalent cation, the negative effect of substituting sulfur for that oxygen should be alleviated if the self-cleavage reaction is performed in the presence of Mn^{2+}, because, unlike hard metal ions such as Mg^{2+}, Mn^{2+} can be coordinated by sulfur (31,32). The black bars in Figure 4 show the effects of thiophosphate substitutions in EHH-c4 transcripts when self-cleavage was performed in the presence of Mn^{2+}. Although the overall pattern of relative intensity ratios is very similar to that generated in the presence of Mg^{2+}, the ratios at almost every position differ slightly. Because of this inherent variation, we cannot conclude that the reductions in the presence of Mn^{2+} of the relatively minor effects at positions UL2.3 and A11.5 indicate divalent cation binding sites, but it is clear that the critically important oxygen adjacent to AL2.2 is not involved in divalent cation binding because the negative effect of substituting sulfur at this position was even more pronounced in the presence of Mn^{2+}. This result differs from the finding at the other critically important position, A9. In the presence of Mn^{2+}, the relative intensity ratio for this position is a little over half of the ratio measured in the presence of Mg^{2+}. Although the absolute value of the ratio is still rather high (4.6), it is common for Mn^{2+} to rescue substitutions at suspected divalent cation binding sites only partially (10,33,34). Despite this evidence that the *pro-R*p phosphate oxygen adjacent to A9 is part of a divalent cation binding site in the extended hammerhead, partial rescue of the A9 position in HH-pt transcripts was not seen in the presence of Mn^{2+} (data not shown). In fact, Mn^{2+} had no obvious effect on any position in HH-pt transcripts (data not shown).

Analysis of a group B extended hammerhead

The chimeric hammerhead domain in EHH-c4 transcripts resembles the group A extended hammerheads found in *N.viri-descens* and several other species from the family Salamandridae. The importance of *pro-R*p oxygens in the peripheral stems of EHH-c4 transcripts prompted us to determine whether similar importance could be assigned to peripheral positions in the group B extended hammerheads. For this purpose we used transcripts that contained the hammerhead domain found in satellite 2 transcripts from *N.maculosus* (Y.Zhang, S.R.Coats and L.M.Eps-tein, unpublished data). This hammerhead has the 6 nt stem II loop that is the most distinguishing feature of the group B extended hammerheads, as well as all of the nucleotides in stems I and II that are conserved in this group (Fig. 6; 18). In our initial experiments we concentrated on stem II and the conserved core of the *N.maculosus* transcripts because most of the important peripheral phosphate oxygens in the EHH-c4 transcripts were found in these regions. Although no substitutions adjacent to C or U residues in these regions affected cleavage (data not shown), several substitutions adjacent to A and G residues did so (Fig.6). These included positions in the conserved core that were similar to the positions identified in both EHH-c4 and HH-pt transcripts, as well as several positions in the terminal portions of stem II. Thus *pro-R*p phosphate oxygens in the external loop of stem II are important for self-cleavage by examples of each of the two extended hammerhead designs.
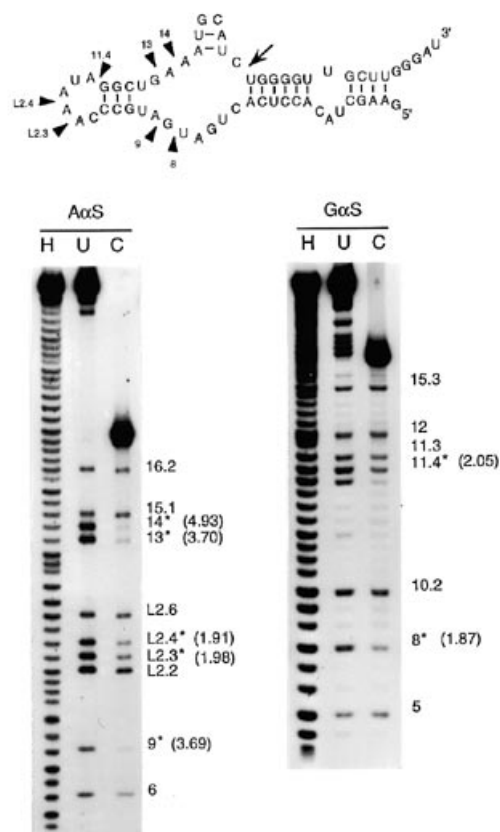

Figure 6. Thiophosphate substitution interference experiments with HH-NecO transcripts. HH-NecO transcripts were prepared using either ATPαS (AαS) or GTPαS (GαS) precursors and analyzed as in Figure 3. Positions investigated are indicated on the right of each gel and span from G5 in the conserved core to A16.2 in stem III. Positions that had intensity ratios >2 SD (1 SD = 0.38) above the group mean of all positions analyzed (1.08) are indicated by an asterisk and their intensity ratios are given in parentheses. These positions are also indicated with arrowheads in the structural model shown at the top.

DISCUSSION

We used a thiophosphate substitution interference analysis to compare the functional requirements in an extended hammerhead of the type found in caudate amphibian satellite 2 transcripts to those in a hammerhead with features similar to those in the prototypical hammerheads found in infectious plant virus RNAs. Four *pro-R*p phosphate oxygens that were important for self-cleavage were found in identical positions in the conserved cores of both hammerhead forms and a fifth was found in similar, although not identical, positions. Three of these positions were identified as important catalytic or structural components in previous studies of prototypical hammerheads. The *pro-R*p phosphate oxygen adjacent to A9 was identified in a previous thiophosphate substitution analysis (9) and was part of a divalent cation binding site in the crystal structure described by Pley *et al*. (5). This latter result is supported by our finding that the inhibitory effect of thiosubstitution at this position in the extended hammerhead was partially alleviated when self-cleavage took place in the presence of Mn^{2+}. In the substituted RNA, the sulfur atom was unable to coordinate Mg^{2+} and self-cleavage was

inhibited, but because sulfur can coordinate Mn^{2+}, self-cleavage was restored when Mn^{2+} was provided. However, the *pro-R*p phosphate oxygen at A9 was not a component of a similar cation binding site found in the prototypical hammerhead crystallized by Scott *et al.* (6). Although both crystal structures used N7 of G10.1 as a coordination point, coordination to A9 in the latter structure was through the *pro-S*p phosphate oxygen. Although the differences in the details of these divalent cation binding sites could have resulted because Pley *et al.* studied the binding of Mn^{2+} and Cd^{2+} to a RNA/DNA hybrid substrate whereas Scott *et al.* studied the binding of Mg^{2+} to a predominantly RNA substrate, they might also reflect an inherent flexibility in the groups used for metal ion binding that allows hammerheads to be active with different peripheral sequences and slightly different tertiary structures. This latter explanation would also accommodate our finding that the inhibitory effect of a substitution at this position in the prototypical hammerhead was not alleviated by the presence of Mn^{2+}.

The other two positions we identified as important, in agreement with the results of previous studies, are the *pro-R*p phosphate oxygens adjacent to A13 and A14. Both were identified in the previous thiophosphate substitution analysis (9) and the phosphate oxygen of A13 was hydrogen bonded to the exocyclic N2 of G8 in the crystal structure of Pley *et al.* (see fig. 4 of ref. 5). This interaction helped to stabilize the non-Watson–Crick base pairing between G8 and A13, which in turn contributed to the coaxial stacking of stems II and III. This indication that the *pro-R*p phosphate oxygen adjacent to A13 is involved in a structural interaction and not in metal ion binding is supported by our finding that Mn^{2+} did not rescue a thiophosphate substitution at this position. It is interesting that in the crystal structure solved by Scott *et al.*, neither of the non-bridging phosphates associated with A13 is positioned to make contact with G8, a further example of the subtle differences in the structures determined in the two crystallographic studies and the subtle effects that peripheral sequences might have on the precise tertiary structure of the conserved core. It seems highly unlikely that all hammerheads use exactly the same functional groups for metal ion binding or for tertiary structural interactions. The slight differences in the positioning of important functional groups in the cores of the extended hammerhead and the various prototypical hammerheads that have been studied can therefore not be taken as proof that these cores fold or are used in dramatically different ways during catalysis. Instead, the similarities in the majority of their important core positions argue that the two hammerhead forms use remarkably similar configurations of the core for catalysis.

Despite the similarities in the core regions of the extended and prototypical hammerheads, the functional groups associated with their peripheral structures significantly differ. No *pro-R*p phosphate oxygens in peripheral regions of the prototypical hammerhead proved important for cleavage or structure formation in this or any previous biochemical or physical study (5,6,9). In fact, active prototypical hammerheads have been formed with and without the terminal loops at the ends of the three stems (35,36) and even when the entire stem II region was replaced with non-helical nucleotide or non-nucleotide linkers (37,38). Nevertheless, five *pro-R*p phosphates were identified as important for cleavage in peripheral regions of the extended hammerhead analyzed here. Although three only slightly exceeded our criterion for importance (A2.7, UL2.3 and A11.5), the other two

(AL2.2 and C11.4) were among the most important positions identified in either hammerhead form analyzed in this study. In fact, thiosubstitution of the *pro-R*p phosphate oxygen of AL2.2 in the external loop of stem II had a greater inhibitory effect than has been seen for any position in any hammerhead form with the exception of the *pro-R*p phosphate oxygen adjacent to the cleavage site (10). That this position was not important in the prototypical hammerhead, even though both hammerhead forms used in this analysis had identical sequences in their stem II regions, strongly suggests that this position is involved in a long range rather than a local interaction. The importance of the stem II region in the extended hammerhead was verified when important *pro-R*p phosphate oxygens were also found in stem II of the hammerhead domain in satellite 2 transcripts from *N.maculosus*. This hammerhead, a group B extended hammerhead, has sequences and structural details in its peripheral stems that distinguish it from the group A extended hammerhead used in the bulk of this analysis (18).

As has been discussed in a slightly different context (39), the different phosphate oxygen requirements in the prototypical and extended hammerheads might simply result from a differential ability to detect similar requirements in reactions that have different rate limiting steps. Although we would have liked to address this issue directly, the stringent requirements in stem–loops II and III of the extended hammerhead preclude the use of a *trans*-cleavage system to dissect the reaction, as has been done for the prototypical form (40,41). Nevertheless, we believe that the reactions investigated in this study have similar rate limiting steps. Because each hammerhead investigated has a core region that conforms to the highly conserved consensus and has functional *pro-R*p phosphate oxygens in conserved positions, the cleavage step is likely to be similar in these and previously investigated hammerheads. Nevertheless, the first order rate constants determined here are almost two orders of magnitude lower than the Michaelis–Menten rate constants determined for prototypical hammerheads, in which the cleavage step was rate limiting (3). Product release cannot be rate limiting in first order reactions where the forward reactions are strongly favored (41) and where the products are analyzed under denaturing conditions. Thus, the reactions are probably inhibited before the cleavage step and the differences observed probably represent differences in precleavage assembly. Because the inhibitory effect of thiophosphate substitution at AL2.2 was not reversed by Mn^{2+}, this position does not appear to be involved in metal ion binding. Instead, it is probably a component of one or more tertiary interactions that help form or stabilize the active structure. These interactions are likely to involve the stem I extension, because we previously showed that active extended hammerheads required compatible combinations of these two stems (23). The existence of specific interactions between stems I and II is entirely feasible because, in the crystal structures of the prototypical hammerheads, stems I and II are roughly parallel and close together (5,6). Thus, it is not surprising that an important *pro-R*p phosphate oxygen was also found in the internal loop of stem I.

Overall, this study supports our earlier proposal that the extended hammerhead is a variant form of the prototypical hammerhead that uses novel tertiary interactions to promote and stabilize the configuration of the same catalytic central core (23). In the prototypical hammerhead, the core is stabilized in part by a rigid backbone formed by coaxial stacking of base pairs in stems II and III (5,6). In both extended hammerhead forms, stem III is

truncated and incapable of contributing to stabilization of the central core. We suggest that in order to compensate for the lack of structural contributions by stem III, interactions have evolved between stems I and II that fix the position of these two stems in the three-dimensional structure and provide a rigid frame for nucleation of the central core. Further studies are necessary to verify this model and to define the nature of these putative interactions. In addition to providing general information about the relationship between structure and function in RNA, these studies could help in the design of maximally stable synthetic hammerheads that combine the interactions between stems I and II used in the extended hammerheads with the interactions between stems II and III used in the prototypical hammerheads.

ACKNOWLEDGEMENTS

REFERENCES

1   Forster,A.C. and Symons,R.H. (1987) *Cell*, **49**, 211–220.
2   Bruening,G. (1989) *Methods Enzymol.*, **180**, 546–558.
3   Long,D.M. and Uhlenbeck,O.C. (1993) *FASEB J.*, **7**, 25–30.
4   Tuschl,T., Gohlke,C., Jovin,T.M., Westhof,E. and Eckstein,F. (1994) *Science*, **266**, 785–789.
5   Pley,H.W., Flaherty,K.M. and McKay,D.B. (1994) *Nature*, **372**, 68–74.
6   Scott,W.G., Finch,J.T. and Klug,A. (1995) *Cell*, **81**, 991–1002.
7   Uhlenbeck,O.C. (1995) *Nature Struct. Biol.*, **2**, 610–614.
8   Ruffner,D.E., Stormo,G.D. and Uhlenbeck,O.C. (1990) *Biochemistry*, **29**, 10695–10702.
9   Ruffner,D.E. and Uhlenbeck,O.C. (1990) *Nucleic Acids Res.*, **18**, 6025–6029.
10 Dahm,S.C. and Uhlenbeck,O.C. (1991) *Biochemistry*, **30**, 9464–9469.
11 Williams,D.M., Pieken,W.A. and Eckstein,F. (1992) *Proc. Natl Acad. Sci. USA*, **89**, 918–921.
12 Yang,J.-H., Usman,N., Chartrand,P. and Cedergren,R. (1992) *Biochemistry*, **31**, 5005–5009.
13 Fu,D.-J., Rajur,S.B. and McLaughlin,L.W. (1993) *Biochemistry*, **32**, 10629–10637.
14 Ng,M.M.P., Benseler,F., Tuschl,T. and Eckstein,F. (1994) *Biochemistry*, **33**, 12119–12126.
15 Epstein,L.M., Mahon,K.A. and Gall,J.G. (1986) *J. Cell Biol.*, **103**, 1137–1144.
16 Cremisi,F., Scarabino,D., Carluccio,M.A., Salvadori,P. and Barsacchi,G. (1992) *Proc. Natl. Acad. Sci. USA*, **89**, 1651–1655.
17 Green,B.A., Pabón-Peña,L.M., Graham,T.A., Peach,S.E., Coats,S.R. and Epstein,L.M. (1993) *Mol. Biol. Evol.*, **10**, 732–750.
18 Zhang,Y. and Epstein,L.M. (1996) *Gene*, **172**, 183–190.
19 Epstein,L.M. and Coats,S.R. (1991) *Gene*, **107**, 213–218.
20 Coats,S.R., Zhang,Y. and Epstein,L.M. (1994) *Nucleic Acids Res.*, **22**, 4697–4704.
21 Epstein,L.M. and Gall,J.G. (1987) *Cell*, **48**, 535–543.
22 Pabón-Peña,L.M., Zhang,Y. and Epstein,L.M. (1991) *Mol. Cell. Biol.*, **11**, 6109–6115.
23 Garrett,T.A., Pabón-Peña,L.M., Gokaldas,N. and Epstein,L.M. (1996) *RNA*, **2**, 699–706.
24 Fedor,M.J. and Uhlenbeck,O.C. (1990) *Proc. Natl. Acad. Sci. USA*, **87**, 1668–1672.
25 Heus,H.A., Uhlenbeck,O.C. and Pardi,A. (1990) *Nucleic Acids Res.*, **18**, 1103–1108.
26 Heidenreich,O., Pieken,W. and Eckstein,F. (1993) *FASEB J.*, **7**, 90–96.
27 Christian,E.L. and Yarus,M. (1992) *J. Mol. Biol.*, **228**, 743–758.
28 Been,M.D., Perrotta,A.T. and Rosenstein,S.P. (1992) *Biochemistry*, **31**, 11843–11852.
29 Griffiths,A.D., Potter,B.V.L. and Eperon,I.C. (1987) *Nucleic Acids Res.*, **15**, 4145–4162.
30 Jeoung,Y., Kumar,P.K.R., Suh,Y., Taira,K. and Nishikawa,S. (1994) *Nucleic Acids Res.*, **22**, 3722–3727.
31 Jaffe,E.K. and Cohn,M. (1979) *J. Biol. Chem.*, **254**, 10839–10845.
32 Eckstein,F. (1985) *Annu. Rev. Biochem.*, **54**, 367–402.
33 Buzayan,J.M., Van Tol,H., Feldstein,P.A. and Bruening,G. (1990) *Nucleic Acids Res.*, **18**, 4447–4451.
34 Christian,E.L. and Yarus,M. (1993) *Biochemistry*, **32**, 4475–4480.
35 Uhlenbeck,O.C. (1987) *Nature*, **328**, 596–600.
36 Haseloff,J. and Gerlach,W.L. (1988) *Nature*, **334**, 585–591.
37 McCall,M.J., Hendry,P. and Jennings,P.A. (1992) *Proc. Natl. Acad. Sci. USA*, **89**, 5710–5714.
38 Hendry,P., Moghaddam,M.J., McCall,M.J., Jennings,P.A., Ebel,S. and Brown,T. (1994) *Biochim. Biophys. Acta*, **1219**, 405–412.
39 Tuschl,T. and Eckstein,F. (1993) *Proc. Natl. Acad. Sci. USA*, **90**, 6991–6994.
40 Fedor,M.J. and Uhlenbeck,O.C. (1992) *Biochemistry*, **31**, 12042–12054.
41 Hertel,K.J., Herschlag,D. and Uhlenbeck,O.C. (1994) *Biochemistry*, **33**, 3374–3385.
42 Hertel,K.J., Pardi,A., Uhlenbeck,O.C., Koizumi,M., Ohtsuka,E., Uesugi,S., Cedergren,R., Eckstein,F., Gerlach,W.L., Hodgson,R. and Symons,R.H. (1992) *Nucleic Acids Res.*, **20**, 3252.